Marcum, J. A., McKenney, J. B., & Rosenberg, R. D. (1984) *J. Clin. Invest. 74*, 341-350.
Marion, D., & Wüthrich, K. (1984) *Biochem. Biophys. Res. Commun. 113*, 967-974.
Mayo, K. H., Holt, J., Rucinski, B., & Niewiarowski, S. (1989) *J. Mol. Biol.* (submitted for publication).
Moore, S., Pepper, D. S., & Cash, J. D. (1975) *Biochim. Biophys. Acta 379*, 379-384.
Patel, D. J., Woodward, C. K., & Bovey, F. A. (1972) *Proc. Natl. Acad. Sci. U.S.A. 69*, 599-602.
Perlmann, G. E., & Longsworth, L. G. (1948) *J. Am. Chem. Soc. 70*, 2719-2724.
Rucinski, B. S., Stewart, G. J., Defeo, P. A., Bodeu, G., & Niewiarowski, S. (1987) *Proc. Soc. Exp. Biol. Med. 186*, 361-367.
Rucinski, B. S., Niewiarowski, S., James, P., Walz, D. A., & Budzynski, A. Z. (1979) *Blood 53*, 47-62.
Senior, R. M., Griffin, G. L., Huang, J. S., Walz, D. A., & Deuel, T. F. (1983) *J. Cell Biol. 96*, 382-385.
St. Charles, R., Walz, D. A., & Edwards, B. F. P. (1989) *J. Biol. Chem. 264*, 2092-2099.
Tanford, C. (1961) *Physical Chemistry of Macromolecules*, pp 286-296 Wiley, New York.
Villaneura, G. B., Allen, N., & Walz, D. A. (1988) *Arch. Biochem. Biophys. 261*, 170-174.
Waddell, W. J. (1956) *J. Lab. Clin. Med. 48*, 311-314.
Walz, D. A., Wu, V. Y., de Lamo, R., Dene, H., & McCoy, L. E. (1977) *Thromb. Res. 11*, 893-898.
Wyman, J. (1964) *Adv. Protein Chem. 19*, 224-250.

Structural and Dynamic Differences between Normal and Transforming N-ras Gene Products: A ^{31}P and Isotope-Edited ^{1}H NMR Study†

Sharon Campbell-Burk‡
Department of Biochemistry, Brandeis University, Waltham, Massachusetts 02254
Received March 29, 1989; Revised Manuscript Received July 21, 1989

ABSTRACT: [^{15}N]Glycine was biosynthetically incorporated into normal cellular N-ras p21 and a position 12 transforming mutant, in order to produce p21 proteins containing several site-specific NMR probes at or near activating positions in the guanine nucleotide binding domain. We have previously assigned all five glycine resonances located in loops directly involved in binding of guanosine diphosphate in the wild-type p21 protein [Campbell-Burk, S., Papastavros, M. Z., McCormick, F., & Redfield, A. G. (1989) *Proc. Natl. Acad. Sci. U.S.A 86*, 817-820]. In this report, the corresponding glycine resonances in the p21 mutant have been assigned, and spectral differences between normal and mutant p21-guanosine diphosphate (p21·GDP) complexes have been investigated. Our combined $^{1}H\{^{15}N\}$ and ^{31}P NMR results show that substitution of aspartate for glycine-12 produces perturbations in the phosphoryl binding domain, near the point of the mutation. Although many of the remaining glycines were unaffected, spectral differences were also observed outside the GDP binding domain. Two of the five active-site glycines in wild-type p21·GDP have very slow amide proton exchange rates with water ($k < 2.8 \times 10^{-5}$ s^{-1}). The active-site glycines are located in solvent-exposed loops, so their apparent solvent inaccessibility may result from strong hydrogen bond formation between glycine amide protons and bound guanine diphosphate and/or other nearby groups in p21.

The most prevalent oncogene found in human cancer belongs to the ras gene family (Nishimura et al., 1987). There are three well-characterized classes of mammalian ras genes (N-ras, K-ras, and H-ras) which encode highly related 21-kDa proteins [for a recent review, see Barbacid (1987)]. p21 proteins are located on the inner surface of the plasma membrane (Willingham et al., 1980; Furth et al., 1983), bind guanine nucleotides with high affinity (Scolnick et al., 1978; Papageorge et al., 1982; Finkel et al., 1984), and possess guanosinetriphosphatase (GTPase) activity (McGrath et al., 1984; Sweet et al., 1984; Gibbs et al., 1984; Manne et al., 1985).

Certain point mutations in the coding sequences of ras genes give rise to p21 proteins capable of inducing transformation-specific phenotypes. Mutant p21 proteins derived from cellular (N-ras) and retroviral (v-H-ras, v-K-ras) ras oncogenes have one to two amino acid substitutions at positions 12, 13, 59, and 61 (Tabin et al., 1982; Reddy et al., 1982; Taparowsky et al., 1982; Yuasa et al., 1983; Bos et al., 1985). These mutant proteins were found to possess lower guanosinetriphosphatase activity relative to their normal cellular homologues (Yuasa et al., 1983; Capon et al., 1983; Reddy et al., 1982). A large number of mutants were produced by site-directed mutagenesis, and their biochemical properties and transformation capabilities were characterized. A correlation was found between mutant proteins capable of stabilizing the GTP-bound conformation and loss in cellular growth control, suggesting that p21·GTP is the biologically active form.

Although the function of p21 proteins is currently unknown despite intensive investigation, similarities between p21 proteins and mammalian G-proteins have led to the hypothesis that p21 proteins may be involved in signal transduction (Halliday, 1984; Gilman, 1987). In analogy with the well-characterized adenylate cyclase regulating G-proteins, G_s and G_i (Gilman,

†This work was partially supported by USPHS Grants 5-F32-GM11847 and GM20168 to S.C.-B. and to A. G. Redfield and by the Cetus Corp.
‡Present address: E. I. du Pont de Nemours and Co., Inc., CR&D, Wilmington, DE 19880-0328.

0006-2960/89/0428-9478$01.50/0

1984, 1987), binding of specific guaning nucleotide substrates (GDP, GTP) is believed to promote association and dissociation of p21 from its targets by generation of an activated enzyme via a GTP-dependent mechanism and inactivation by enzymatic hydrolysis to GDP and inorganic phosphate.

Site-directed mutagenesis studies have identified several domains which are critical for p21 function (Barbacid, 1987). A crystal structure of H-ras p21·GDP has recently been reported (de Vos et al., 1988), showing most of these critical domains or positions to be located in loops which connect α-helix or β-sheet secondary elements. These loops are highly conserved in N-ras and H-ras p21 and contain active-site residues involved in binding of guanine nucleotides, putative molecular recognition sites, and amino acids involved in Y13-259 antibody binding (Sigal et al., 1986). Regions containing loops are generally difficult to define by structural analysis relative to α-helix and β-strand secondary structural elements because they lack predictable periodic structure, are generally located at surface-exposed regions, and have more conformational flexibility. However, these same features, which make structural analyses difficult, may prove important for molecular recognition and binding of ligands.

In our initial studies, [^{15}N]glycine was biosynthetically incorporated into both wild-type p21 and a transforming mutant (Gly-12 → Asp-12) because several glycines are located at or near activating positions in the p21·GDP binding domain (deVos et al., 1988). With the use of isotope-edited 1D and 2D NMR techniques [reviewed in Griffey and Redfield (1987)], the 14 glycine resonances were filtered out from over 1000 proton resonances, providing considerable spectral simplification. All five glycine residues located in GDP binding loops were previously identified in wild-type p21·GDP (Campbell-Burk et al., 1989) using proton-edited NMR techniques.

We report here the assignment of several active-site glycines resonances in an Asp-12 transforming mutant and ^{31}P and isotope-edited NMR results obtained from studying spectral differences between normal and mutant p21 proteins complexed to guanosine diphosphate.

Materials and Methods

Production of [^{15}N]Glycine-Enriched p21 Proteins. [^{15}N]Glycine-enriched N-ras p21 and [^{15}N]glycine Asp-12/p21 proteins were produced as previously described (Campbell-Burk et al., 1989). Guanosine diphosphate was obtained from Boehringer Mannheim and used without further purification.

GTPase Assay. GTPase activity of p21 proteins was determined by using a radioassay similar to that of Manne et al. (1984). The standard assay reaction mixture consisted of 10 μg/mL p21, 2.5 mM GTP (95 pmol of [γ-^{32}P]GTP, ~5000 Ci/mmol), 50 mM tris(hydroxymethyl)aminomethane, 5 mM $MgCl_2$, and 2 mM dithiothreitol, pH 7.5, 37 °C, in a total volume of 0.2 mL. Aliquots (0.04 mL) of the reaction mixture were taken at different times and quenched in an ice-cold solution containing 0.05 mL of 6 M HCl, 0.15 mL of 3.75% $(NH_4)_6MO_7O_{24}$, and 0.3 mL of butyl acetate, 0 °C. The quenched reaction mixture was vortexed for 30 s and centrifuged at 5000 rpm in a clinical centrifuge. One hundred microliters of the organic phase was added to 10 mL of scintillation fluid (Opti-fluor, Packard) and counted using a Beckman scintillation counter. Protein concentration was determined by using the Bio-Rad assay.

NMR Spectroscopy. Samples (10–20 mg) for NMR analysis were prepared by dialysis against 50 mM NaCl, 5 mM $MgCl_2$, 0.2 mM dithiothreitol, and 0.02% sodium azide with either 20 mM Tris, pH 7.5, or 50 mM borate, pH 8.2. The samples were then concentrated at low pressure in an Amicon Model 8010 with a Diaflo YM10 membrane, followed by further concentration to about 0.4 mL with Amicon Centricon 10 cartridges. D_2O (Bio-Rad, biochemical grade) was added to 10% for NMR lock.

Exchange of NMR samples into a D_2O-based buffer was accomplished by using a Quik-sep column (Isolab Inc., Akron, OH). Sephadex G-25 resin was equilibrated with NMR buffer prepared in D_2O, and 2.5 mL was added to the spin column. The excess solvent was quickly spun out using a rotating-bucket centrifuge. The excluded solvent was then removed by a second spin at full speed for 90 s. Up to 450 μL of protein sample was added and spun again for 60–90 s at full speed, and the effluent protein was collected for NMR analysis.

Proton–^{15}N 2D correlation or HMQC (Bax et al., 1983; Griffey & Redfield, 1987) and edited nuclear Overhauser effect (NOE) experiments were performed as described previously (Griffey & Redfield, 1987; McIntosh et al., 1987; Campbell-Burk et al., 1989), on a home-built 500-MHz spectrometer and using a quadruply tuned probe supplied by Cryomagnet Systems. Data were transformed on an IBM AT compatible microcomputer with minor preweighting to reduce H_2O noise and to optimize resolution. The data were then transferred to a VAX computer for plotting using software kindly supplied by Hare Software (Woodinville, WA). ^{31}P NMR measurements were performed on a Varian XL 300-MHz spectrometer at 121.416 MHz.

Results

^{1}H–^{15}N 2D Map of Wild-Type p21·GDP. The HMQC (heteronuclear multiple quantum correlation) spectrum of wild-type [^{15}N]glycine-enriched N-ras p21 proteins is displayed in the left panel of Figure 1. All 14 peaks are resolved in the 2D map shown, with each peak corresponding to a single glycine amide (^{15}NH) group in wild-type p21. [^{15}N]Glycine chemical shifts are obtained by extrapolation down to the horizontal axis, while the glycine amide proton resonance frequencies can be read from the vertical axis.

All five glycine residues located in the guanosine diphosphate binding domain of wild-type p21·GDP have previously been identified (Campbell-Burk et al., 1989) with resonances A, F, K, L, and N in Figure 1. Three of these glycines resonances (A, F, and K), were collectively assigned to glycines at positions 10, 15, and 115. Gly-12 and Gly-13 were assigned to peaks L and N, respectively.

Glycine amide proton resonances B, F, and K were the only three resonances observed in a HMQC map of Gly-12 p21·GDP, 10 h after p21 was transferred to a D_2O-based buffer (Table I). These resonances correspond to 3 glycine residues in p21·GDP whose amide protons exchange slowly with water ($k < 2.8 \times 10^{-5}$ s^{-1}), relative to the other 11 glycines in p21. Two of the three slowly exchanging amide protons were identified as active-site glycine peaks (F and K).

Comparison of Normal and Transforming Mutant p21·GDP ^{1}H–^{15}N 2D Maps. The transforming mutant was originally cloned from a patient with acute myelocytic leukemia (Gambke et al., 1985) and encodes a 21-kD protein containing aspartate instead of glycine at position 12. The GTPase activities of normal and mutant p21 proteins were found to be similar to those reported by Trahey et al. (1987), with Asp-12 p21 retaining approximately 50% of wild-type GTPase activity. The GTPase activity of normal and mutant p21 proteins did not vary over the course of the NMR measurements.

Comparison of normal and transforming mutant 2D maps shows both chemical shift as well as intensity variations in

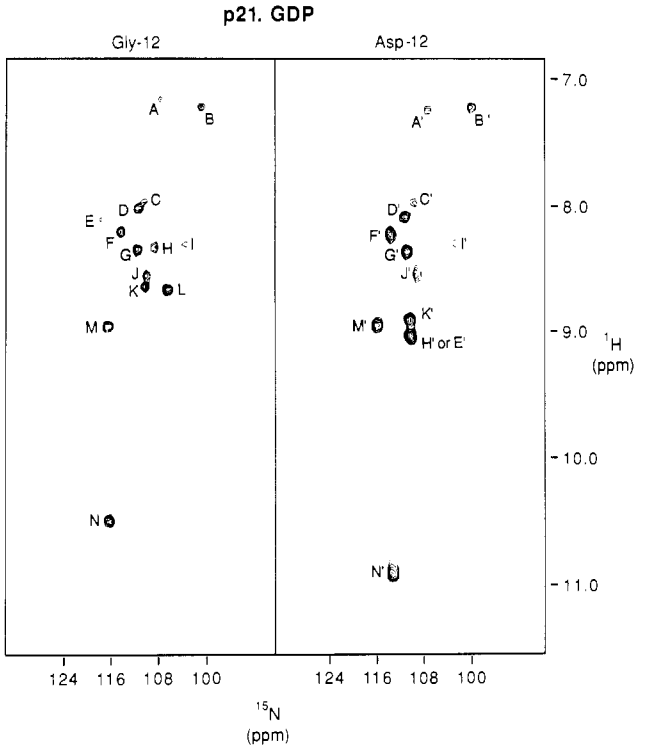

FIGURE 1: Proton–^{15}N correlation spectra of [^{15}N]glycine N-ras p21 (left) and mutant (Asp-12) [^{15}N]glycine-enriched N-ras p21 (right). p21 samples consisted of ~2 mM protein in 20 mM Tris, 40 mM NaCl, 5 mM $MgCl_2$, 0.2 mM DTT, 10% D_2O, and 0.02% Az. The spectrum was recorded at 22 °C, essentially as described by McIntosh et al. (1987a,b). Spectra were acquired using a total of 128 t_1 with 16 t_1/cycle. Six complete cycles of 512 free induction decays and 512 total points were collected in 9 h. The proton sweep width was 512 kHz, and the ^{15}N sweep width was 5.0 kHz. The data were zero-filled 2-fold and complex Fourier transformed, with mild Gaussian convolution flattening and line broadening in both directions.

Table I: ^{1}H–^{15}N Heteronuclear 2D Chemical Shift Data

		Gly-12 p21·GDP			Asp-12 p21·GDP	
peak	Gly position	^{1}H	^{15}N	peak	^{1}H	^{15}N
A	10, 15, 115	7.13	108.0	A′	7.22	108.3
B		7.18[a]	101.8	B′	7.21[a]	101.6
C		7.94	110.5	C′	7.96	110.5
D		7.99	111.2	D′	8.06	111.8
E		8.10	117.4	E′	[9.02	111.0][b]
F	10, 15, 115	8.19[a]	114.1	F′	8.20[a]	114.1
G		8.33	111.4	G′	8.34[a]	111.8
H	[60][c]	8.31	108.7	H′	[9.02	111.0][b]
I		8.29	104.1	I′	8.29	104.1
J		8.52	110.3	J′	8.55	110.1
K	10, 15, 115	8.60[a]	110.3	K′	8.92	111.0
L	12	8.64	107.0			
M		8.92	115.8	M′	8.94	116.0
N	13	10.48	115.8	N′	10.94	113.9

[a] Slowly exchanging amide protons. [b] Resonance may correspond to either E′ or H′. [c] Probable assignment for Gly-60 NH resonance.

several peaks (Figure 1). The mutant contains aspartate instead of glycine at position 12 so its HMQC map contains one fewer glycine resonance. The chemical shifts of glycine ^{15}NH resonances are listed in Table I, with wild-type p21·GDP glycine chemical shifts designated as A–N, and Asp-12 p21·GDP resonances, A′–N′. All four glycine resonances (A′, F′, K′, N′) in the GDP binding site of Asp-12/p21 were assigned as described below.

There are three Val-Gly pairs (Val9-Gly10, Val14-Gly15, and Val114-Gly115) in the sequence of normal and mutant p21. HMQC spectra of a doubly labeled p21 sample containing both [1-^{13}C]valine and [^{15}N]glycine allowed active-site resonances corresponding to Gly-10, -15, and -115 in wild-type p21 to be collectively identified (Campbell-Burk et al., 1989). These assignments were made by observing changes in the line width of [^{15}N]glycine resonances in heteronuclear correlation 2D maps of doubly labeled [1-^{13}C]valine/[^{15}N]glycine before and after ^{13}C decoupling of carbonyl amide splittings.

In a similar manner, HMQC spectra of Asp-12/p21·GDP doubly labeled with [1-^{13}C]valine and [^{15}N]glycine were recorded (Figure 2). The ^{13}C nucleus splits glycine ^{15}NH resonances of the three glycine residues which possess valine N-terminal neighbors (Gly-10, -15, and -115). Since the coupling constant is on the order of the line width (~15 Hz), peak broadening rather than splitting is observed in the ^{15}N dimension of Figure 2a. Inspection of Figure 2a shows resonances A′, F′, and K′ broadened due to the $J(^{13}C–^{15}N)$ coupling interaction. The HMQC spectrum acquired with monochromatic radiofrequency irradiation applied to the ^{13}C amide region is displayed in Figure 2b. Peaks labeled A′, F′, and K′ show increased intensity and narrower line widths in the ^{15}N dimension relative to Figure 2a, due to collapse of J coupling between [^{13}C]Val/[^{15}N]Gly.

These measurements do not provide individual assignments for glycines-10, -15, and -115 (collectively assigned to A′, F′, and K′), because all three glycine residues share a valine N-terminal neighbor. The resonance at 8.2, 114.1 ppm was assigned to F′ since its chemical shift is identical with glycine peak F in the wild-type HMQC 2D spectrum. Similarly, A′ was assigned to the peak at 7.1, 108.0 ppm since its chemical shift is similar to resonance A in wild-type p21 (7.1, 108.0 ppm). By difference, the peak at 8.9, 111.0 ppm was assigned to K′.

Further confirmation of A′, K′ assignments was obtained by use of a one-dimensional isotope-edited NOE experiment. This NMR technique (Griffey & Redfield, 1987) selects for nuclear Overhauser effects from only a single preselected amide proton residing on a ^{15}N-labeled nitrogen. The edited NOE experiment is similar to ordinary 1D NOE measurements but uses predecoupling of ^{15}N frequencies, guided by the chemical shift information from 2D maps such as Figure 1. This method was previously used to assign Gly-12 and Gly-13 NH resonances in wild-type p21·GDP (Campbell-Burk et al., 1989).

The downfield region (7–11 ppm; ^{1}H) of wild-type and mutant isotope-edited NOE difference spectra, produced by selective irradiation of nitrogen and proton resonance frequencies of peaks K and K′, is shown in the top and bottom of Figure 3a, respectively. Identical downfield NOE peaks are generated by irradiation of K and K′, indicating that they arise from the same glycine residue. Thus, the resonance at 8.6, 110 ppm (K) in wild-type p21·GDP appears to shift to 8.9, 110 ppm (K′) in the transforming mutant.

Nuclear Overhauser effects characteristic of a valine spin system were observed in the upfield region (not shown), indicating that K and K′ are within 5 Å from a valine side chain. An isotope-edited NOE difference spectrum of Asp-12 p21·GDP, produced by selective irradiation of A′ at 7.2, 108 ppm (^{1}H, ^{15}N ppm), is shown in Figure 3b. Strong upfield NOEs unique to valine C_β-methine and C_γ-methyl protons are observed. These results are consistent with our assignments of A′ and K′ obtained on a doubly [1-^{13}C]Val, [^{15}N]Gly mutant ras sample.

The resonance corresponding to glycine-13, located next to the point of mutation, was assigned by comparison of wild-type and mutant ras–p21 2D maps after identification of resonances

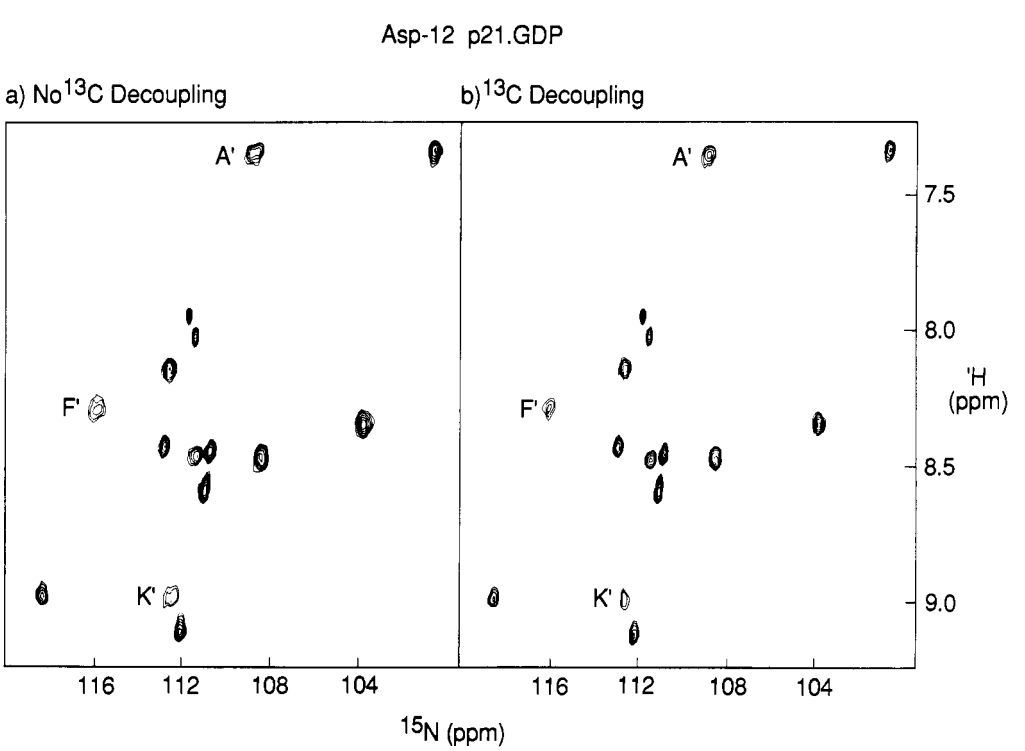

FIGURE 2: (a) HMQC spectrum of Asp-12/p21·GDP doubly labeled ([1-^{13}C]valine and [^{15}N]glycine). Data were acquired with 4-fold increased resolution in the ^{15}N dimension and 2-fold increased resolution in the ^{1}H dimension relative to Figure 1. (b) HMQC spectrum of [1-^{13}C]-valine/[^{15}N]glycine-labeled Asp-12/p21·GDP acquired as described in (a) except that radiofrequency irradiation was applied at the ^{13}C-peptide carbonyl region, to collapse the [1-^{13}C]Val/[^{15}N]Gly coupling interaction as described previously (Campbell-Burk et al., 1989). Resonances A′, F′, and K′ have higher intensity and decreased line widths in the ^{15}N dimension relative to (a), while the line width of the other resonances is not affected by ^{13}C irradiation.

A′, F′, and K′. Peak N was identified as Gly-13 in the wild-type p21·GDP 2D map. This glycine resonance has an unusual chemical shift, 10.48, 115.8 ppm (^{1}H, ^{15}N ppm) in the 2D spectrum of wild-type p21 and was replaced by a peak in the Asp-12 mutant that was sufficiently close to its position in the normal protein (10.94, 113.9 ppm) that we assumed it arose from the same residue. Resonances N and N′ decrease significantly in intensity when guanosine diphosphate is partially removed from the protein.

The peak positions of three (A, K, N) out of four (A, F, K, N) active-site glycine resonances differ between wild-type and mutant p21·GDP 2D maps. A small shift was also observed for peak D. Although this resonance (D) has not yet been assigned, it corresponds to a glycine residue located outside the loops directly involved in GDP binding, since all of the glycines located in the GDP binding site have been assigned.

Further inspection of normal and mutant 2D maps shows additional spectral differences. We did not observe a resonance at 8.3, 108 ppm (^{1}H, ^{15}N), the peak position of resonance H in the wild-type p21 spectrum. A probable assignment for resonance H is glycine-60, because a large edited NOE was observed from peak H in wild-type p21·GDP to a resonance at 1.3 ppm (data not shown), which may correspond to the Ala-59 methyl. Glycine-60 is believed to be located in a β-turn, near the γ-phosphate of GTP in a p21·GTP complex (de Vos et al., 1988), so there is a high probability of seeing an NOE between the Ala-59 methyl and Gly-60 NH. The only other glycine resonance with an alanine N-terminal neighbor is Gly-12, which has already been assigned. It is likely that resonance H shifts from 8.3, 108 to 9.02, 111 ppm in the mutant spectrum. A large isotope-edited NOE at 1.5 ppm was observed upon irradiation of the resonance at 9.02, 111 ppm, suggesting that this glycine NH may be near (<5 Å) an alanine methyl in mutant p21·GDP. However, a resonance at the position of E in the wild-type p21·GDP ^{1}H–^{15}N 2D map is not observed in the mutant spectrum. Therefore, the resonance at position 9.02, 111 ppm may be either H or E. One of these two peaks is either shifted under another glycine peak or decreases in intensity, so that it is not detectable in the mutant spectrum shown. We expect to resolve this assignment by generation of a [1-^{13}C]Ala/[^{15}N]glycine doubly labeled sample.

Table II: ^{31}P NMR Chemical Shifts (ppm)

complex	α	β
Mg·GDP	−9.9	−5.8
p21·Mg·GDP	−10.5	−1.8
Asp-12 p21·Mg·GDP	−11.4	−2.9

^{31}P NMR of α- and β-Phosphate Resonances of Mg·GDP, Gly-12 p21·GDP, and Asp-12 p21·GDP. ^{31}P NMR spectra of free Mg·GDP, Gly-12/p21·Mg·GDP, and Asp-12/p21·GDP are shown in Figure 4a–c. Inspection of Figure 4a,b shows a large upfield displacement in the position of the GDP β-phosphate in the spectrum of Gly-12/p21·GDP relative to free Mg·GDP. The α-phosphate undergoes a much smaller downfield shift. Chemical shift values for α- and β-phosphate resonances of GDP are listed in Table II. The line widths of the bound phosphates are larger than those of free Mg·GDP (Figure 4a) as expected from the increased rotational correlation time of the protein–nucleotide complex.

The mutant ^{31}P NMR spectrum of p21·GDP (Figure 4c) differs from that of wild-type p21·GDP (Figure 4b). Both α- and β-phosphate resonances in the Asp-12/p21·GDP complex shift downfield relative to Gly-12/p21·GDP phosphate peaks. The chemical shifts of Asp-12/p21·GDP also differ from free Mg·GDP. The α-phosphate of Asp-12/p21·GDP is shifted downfield by 1.5 ppm relative to free Mg·GDP whereas the β-phosphate is shifted 2.9 ppm upfield from the β-phosphate resonance of Mg·GDP.

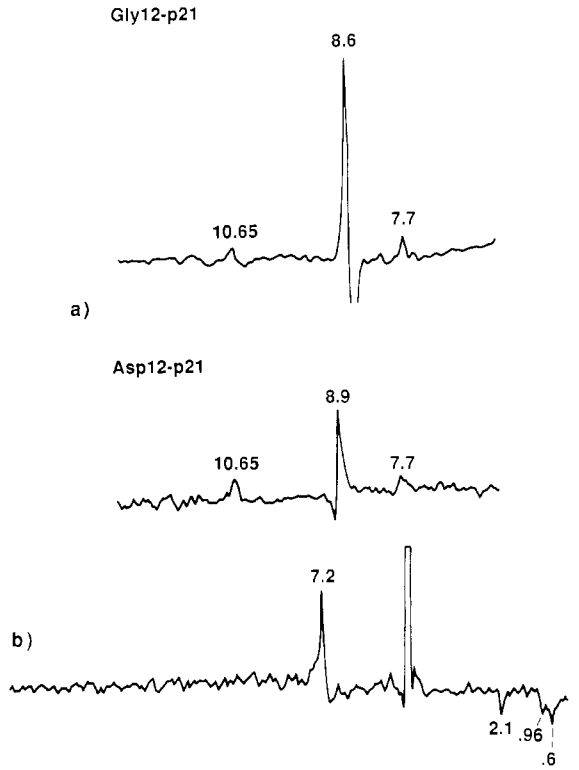

FIGURE 3: (a) Comparison of wild-type (top) and mutant (bottom) isotope-directed NOE difference spectra. Both glycine amide proton resonances have common downfield NOEs as shown. The resonance at 8.6, 110 ppm in wild-type p21·GDP appears to shift to 8.9, 110 ppm (K) in the transforming mutant. (b) Isotope-directed NOE difference Asp-12/p21·GDP. Spectra were acquired as described in McIntosh et al. (1987a,b). Selective preirradiation of resonance A [7.2, 108 ppm (^{1}H, ^{15}N) ppm] shows strong upfield NOEs unique to valine C_β-methine and C_γ-methyl protons. The C_β-methine and C_γ-methyl protons are inverted because the J–R 90° pulse, used to selectively excite the amide proton region, produces an excitation profile which has a null at the water resonance (for solvent suppression) and is 180° out of phase upfield from water (Redfield, 1986; Plateau & Gueron, 1982). An isotope-directed NOE experiment was performed on peak A in the normal protein and gave similar upfield NOEs characteristic of the valine spin system. Peak A in the normal protein was assigned by preparation of a doubly labeled protein sample ([1-^{13}C]valine, [^{15}N]glycine).

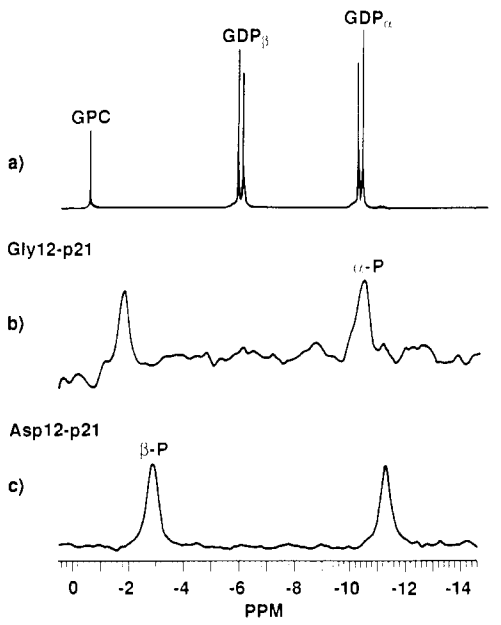

FIGURE 4: ^{31}P NMR spectra of (a) free Mg·GDP, (b) p21·Mg·GDP, and (c) Asp-12/p21·Mg·GDP. Sample conditions are as in Figure 1. Chemical shifts are given using glycerophosphocholine as an internal reference (−0.49 ppm; H_3PO_4 = 0.0 ppm). A 45° pulse and 3-s relaxation delay were used to acquire spectra.

DISCUSSION

We have identified several glycine resonances in 2D maps of [^{15}N]glycine-enriched normal and mutant p21 proteins. Of the 14 glycine residues in p21, all 5 resonances corresponding to glycines in GDP binding loops have been identified, and a preliminary assignment for Gly-60 was obtained. Spectral differences between normal p21 and an Asp-12/p21 transforming mutant complexed to GDP were monitored by using glycine resonances as site-specific probes.

The crystal structure of H-ras p21·GDP has identified the GDP binding site (de Vos et al., 1988; Tong et al., 1989). Although the N-ras p21·GDP crystal structure has not been solved, the amino acid sequences in the N-terminal domain of N-ras and H-ras p21 are practically identical (Wigler, 1984), making it possible to draw structural correlations between the N-terminal domain of H- and N-ras p21·GDP.

Our [^{15}N]glycine spectral probes are located in the following domains. A glycine-rich loop in the phosphoryl binding domain contains glycines-10, -12, -13, and -15. Glycine-60 is located in a loop near the glycine-rich phosphoryl binding loop and is believed to be near the γ-phosphate of GTP in p21·GTP complexes. Glycine-115 is located in one of the two loops which form a side of the pocket for the guanine nucleotide base.

Miscoding mutations in residues 12, 13, 15, 16, 61, 63, 116, and 119 result in oncogenic activation of ras genes [reviewed in Barbacid (1987)]. These activating positions are located at or near glycine probes at positions 10, 12, 13, 15, 60, and 115. Certain mutations in the phosphoryl binding domain near glycines 10, 12, 13, 15, and 60 give rise to altered proteins with impaired GTPase activity and transforming-inducing properties, whereas p21 proteins with mutations in regions involved in binding of the guanine nucleotide base (near glycine-115) show increased guanine nucleotide exchange rates. The activating mutations are believed to stabilize the p21·GTP conformation in vivo. This activated p21 state is believed to be a necessary intermediate in the recognition and modulation of the activity of a target enzyme, which through a series of events (signal transduction) leads to regulation (wild-type p21) or loss of cellular growth control (ras–oncogene p21 products).

There are three slowly exchanging glycine amide proton resonances in Gly-12/p21·GDP. Two of these slowly exchanging amide proton resonances correspond to glycines located in the GDP binding domain. Protons which do not exchange in aqueous solution are often located in the interior of the protein and/or correspond to protons which form hydrogen bonds, such as those necessary to stabilize α-helix or β-sheet secondary structures. The crystal structure of H-ras p21·GDP revealed that the two loops containing Gly-10, -12, -13, -15, and -115 are exposed at the surface of the protein (deVos et al., 1988), so it is likely that strong hydrogen bond formation between these glycine amide proton resonances and other p21 residues or bound substrates prevents exchange with D_2O. These observations are particularly interesting because they indicate that the glycine-rich phosphoryl binding loop may form tight associations in p21·GDP and may be conformationally restrained, rather than highly flexible and capable of adopting several conformations (Fry et al., 1986; Pincus & Scheraga, 1985).

A significant NOE (~10%) was observed between Gly-12 and Gly-13, indicating that the glycine amide protons are less than 5 Å from each other (Campbell-Burk et al., 1989). Sequential NOEs between two amide protons are generally

not observed in parallel or antiparallel β-sheet secondary structures, but are observed in α-helix, 3_{10}-helix, and type I and II turns. Since Gly-12 and Gly-13 are located in the middle of the phosphoryl binding loop in H-ras p21·GDP, it is likely that the conformation of the loop near these glycines more closely resembles a turn than an extended loop. These results are consistent with the structure of the glycine-rich loop determined by X-ray crystallography (deVos et al., 1988) as predicted earlier by McCormick et al. (1985).

Results from our $^{1}H\{^{15}N\}$ studies of p21·GDP and Asp-12/p21·GDP indicate a perturbation in the phosphoryl binding domain when aspartate is substituted for glycine at position 12. The peak positions of three out of four glycine NH resonances, assigned to glycines residues located in the guanine nucleotide binding domain, differ between normal and mutant 2D spectra.

Glycine-60 is located in a β-turn near the glycine-rich loop in the phosphoryl binding domain and is believed to be near the γ-phosphate of GTP in the p21·GTP complex (de Vos et al., 1988). The chemical environment of a glycine resonance believed to be glycine-60 is also perturbed by the aspartate substitution at position 12.

The position 12 mutation affects the chemical environment of α- and β-phosphates of bound GDP as well as glycine residues located near the phosphates, since our ^{31}P NMR results indicate that the chemical environment of both α- and β-phosphates in p21·GDP complexes differs in normal and transforming mutant p21·GDP. In the H-ras p21·GDP crystal structure, the β-phosphate of GDP is located just above the glycine-rich loop (glycines-10, -12, -13, and -15).

A small shift is also observed in a resonance (D) which corresponds to a glycine residue located outside the loops involved in binding of GDP. Furthermore, since we were not able to assign resonance E in the mutant spectrum, our results indicate that the Asp-12 mutation appears to affect one or more regions outside the GDP binding domain in addition to the GDP binding domain. However, the mutation does not produce a global perturbation in p21 structure since six glycines dispersed throughout the protein are not affected by the Asp-12 substitution.

The Asp-12 substitution does not appear to confer temperature sensitivity to p21 (i.e., morphological transformation, GTPase activity, GDP binding, susceptibility to proteolysis), so it is unlikely that generation of a temperature-sensitive mutant is responsible for the observed glycine NH chemical shift differences in normal and mutant 2D spectra. Furthermore, none of the active-site glycine resonances displayed a large chemical shift dependence as a function of temperature over a range of 4–37 °C. The observed perturbations in the chemical shifts of these resonances may result from a conformational change in the phosphoryl binding domain or a more localized perturbation in the chemical environment of glycine amide groups positioned near the mutation.

It is not surprising that the amino acid substitution produces perturbations in glycine amide resonances residing in the phosphoryl binding domain, since Gly-12 is replaced by a larger acidic amino acid in a loop containing several hydrophobic amino acids. However, substitution of glycine-12 for any amino acid except proline produces transformation-active p21 proteins. It is likely that conformational changes, produced by various amino acid substitutions, will depend on the substitution and that glycine-12 or proline-12 is critical for stabilization of the conformation which represents the inactive state of p21 in vivo.

A report of the crystal structure of H-ras p21·GDP and Val-12/p21·GDP refined to 2.2-Å resolution has recently appeared in the literature (Tong et al., 1989). Structural changes in loops 1 and 4 between normal and Val-12 H-ras/p21·GDP were observed, consistent with our NMR comparison of N-ras/Gly-12 p21·GDP and N-ras/Asp-12 p21·GDP.

In summary, our results demonstrate the potential of isotope-edited NMR to investigate domains in larger proteins (>20 kDa). This NMR approach can be used to rapidly assess perturbations at or around specific sites or domains, due to point mutations or binding of ligands, in a way that complements crystallographic studies. Further NMR studies should provide additional information concerning relative structural and dynamic changes between normal and transforming mutant p21 proteins, in addition to ligand-induced (GTP vs GDP) changes (unpublished results). In addition, studies of this type may provide valuable information not only of molecular details which contribute to biological transformation but also of the activation process common to homologous G-proteins which play a role in signal transduction.

Acknowledgments

I am indebted to Dr. Alfred Redfield, who sponsored this research effort, for helpful technical and scientific advice during the course of this work. I gratefully acknowledge Frank McCormick for supplying the N-ras clones and biochemical information regarding p21 proteins derived from these clones. I thank Katherine Hall, Taro Fujimori, Mary Papastavros, and Meg Trahey for many helpful discussions and biochemical assistance.

Registry No. Glycine, 56-40-6.

References

Barbacid, M. (1987) *Annu. Rev. Biochem. 56*, 799–827.
Bax, A., Griffey, R. H., & Hawkins, B. L. (1983) *J. Magn. Reson. 55*, 301–335.
Bos, J. L., Toksoz, D., Marshall, C. J., Verlaan-de Vries, M., Veeneman, G. H., van der Eb, A. J., van Boom, J. H., Janssen, J. W. G., & Steenvoorden, A. C. M. (1985) *Nature 315*, 726–730.
Campbell-Burk, S., Papastavros, M. Z., McCormick, F., & Redfield, A. G. (1989) *Proc. Natl. Acad. Sci. U.S.A. 86*, 817–820.
Capon, D. J., Seeburg, P. H., McGrath, J. P., Hayflick, J. S., Edman, U., Levinson, A. D., & Goeddel, D. V. (1983) *Nature 304*, 507–513.
Cohn, M. (1979) *NMR and Biochemistry* (Opella, S. J., & Lu, P., Eds.) Marcel Dekker, New York.
deVos, A. M., Tong, L., Milburn, M. V., Matias, P. M., Jancarik, J., Noguchi, S., Nishimura, S., Miura, K., Ohtsuka, D., & Kim, S.-H. (1988) *Science 239*, 888–893.
Finkel, T., Der, C. J., & Cooper, G. M. (1984) *Cell 37*, 151–158.
Fry, D. C., Kuby, S. A., & Mildvan, A. S. (1986) *Proc. Natl. Acad. Sci. U.S.A. 83*, 907–911.
Furth, M. E., Davis, L. J., Fleurdelys, B., & Scolnick, E. M. (1982) *J. Virol. 43*, 294–304.
Gambke, C., Hall, A., & Moroni, C. (1985) *Proc. Natl. Acad. Sci. U.S.A. 82*, 879–882.
Gibbs, J. B., Sigal, I. S., Poe, M., & Scolnick, E. M. (1984) *Proc. Natl. Acad. Sci. U.S.A. 81*, 5704–5708.
Gilman, A. G. (1984) *Cell (Cambridge, Mass.) 36*, 577–579.
Gilman, A. G. (1987) *Annu. Rev. Biochem. 56*, 615–649.
Griffey, R. H., & Redfield, A. G. (1987) *Q. Rev. Biophys. 19*, 51–82.

Griffey, R. H., Redfield, A. G., Loomis, R. E., & Dahlquist, F. W. (1985) *Biochemistry 24*, 817-822.
Halliday, K. R. (1984) *J. Cyclic Nucleotide Protein Phosphorylation Res. 9(6)*, 435-448.
Manne, V., Bekesi, E., & Kung, H.-F. (1984) *Proc. Natl. Acad. Sci. U.S.A. 82*, 376-380.
McCormick, F., Clark, B. F. C., LaCour, T. F. M., Kjeldgaard, M., Norskov-Lauritsen, L., & Nyborg, J. (1985) *Science 238*, 78-82.
McGrath, H. P., Capon, D. J., Goeddel, D. V., & Levinson, A. D. (1984) *Nature (London) 310*, 644-649.
McIntosh, L. P., Dahlquist, F. W., & Redfield, A. G. (1987a) *J. Biomol. Struct. Dyn. 5*, 21-34.
McIntosh, L. P., Griffey, R. H., Muchmore, D. C., Nelson, C. P., Redfield, A. G., & Dahlquist, F. W. (1987b) *Proc. Natl. Acad. Sci. U.S.A. 84*, 1244-1248.
Mildvan, A. S. (1987) *Magnesium 6*, 28-33.
Nakano, A., Miyazawa, T., Nakamura, S., & Kaziro, Y. (1980) *FEBS Lett. 116*, 72-74.
Nishimura, S., & Sekiya, T. (1987) *Biochem. J. 243*, 313.
Papageorge, A., Lowy, D., & Scolnick, E. M. (1982) *J. Virol. 44*, 509-519.
Pincus, M. R., & Scheraga, H. A. (1985) *Acc. Chem. Res. 18*, 372-379.
Plateau, P., & Gueron, M. (1982) *J. Am. Chem. Soc. 104*, 7310-7311.
Reddy, E. P., Reynolds, R. K., Santos, E., & Barbacid, M. (1982) *Nature 300*, 149-152.
Redfield, A. G. (1986) *NATO ASI Ser., Ser. A 107*, 1-10.
Rosch, P., Whittinghofer, A., Tucker, J., Sczakiel, G., Leberman, R., & Schlichting, I. (1986) *Biochem. Biophys. Res. Commun. 135*, 549-555.
Scolnick, E. M., Papageorge, A. G., & Shih, T. Y. (1979) *Proc. Natl. Acad. Sci. U.S.A. 76*, 5355-5359.
Sigal, I. S., Gibbs, J. B., D'Alonzo, J. S., & Scolnick, E. M. (1986) *Proc. Natl. Acad. Sci. U.S.A. 83*, 4725-4729.
Sweet, R. W., Yoloyama, S., Kamata, T., Feramisco, J. R., Rosenberg, M., & Gross, M. (1984) *Nature (London) 311*, 273-275.
Tabin, C. J., Bradley, S. M., Bargmann, C., Weinberg, R. A., Papageorge, A. G., Scolnick, E. M., Dhar, R., Lowy, D. R., & Change, E. H. (1982) *Nature 300*, 143-149.
Taparowsky, E., Suard, Y., Fasano, O., Shimizu, K., Goldfarb, M., & Wigler, M. (1982) *Nature 300*, 762-765.
Tong, L., de Vos, A. M., Milburn, M. V., Jancarik, J., Noguchi, S., Nishimura, S., Miura, K., Ohtsuka, E., & Kim, S.-H. (1989) *Nature 337*, 90-93.
Trahey, M., Miller, R. J., Cole, G. E., Innis, R. M., Patterson, H., Marshal, C. J., Hall, A., & McCormick, F. (1987) *Mol. Cell. Biol. 7*, 541-544.
Wigler, M., Fasano, O., Taparowsky, E., Powers, S., Kataoka, T., Birnbaum, D., Shimizu, K., & Goldfarb, M. (1984) *Cancer Cells 2*, 419-423.
Willingham, M. C., Pastan, I., Shih, T. Y., & Scolnick, E. M. (1980) *Cell 19*, 1005-1014.
Wittinghofer, A., Goody, R. S., Rosch, P., & Kalbitzer, H. R. (1982) *Eur. J. Biochem. 124*, 109-115.
Yuasa, Y., Srivastava, S. K., Dunn, C. Y., Rhim, J. S., Reddy, E. P., & Aaronson, S. A. (1983) *Nature 303*, 775-779.

Sequence- and Structure-Dependent DNA Base Dynamics: Synthesis, Structure, and Dynamics of Site and Sequence Specifically Spin-Labeled DNA†

Andreas Spaltenstein, Bruce H. Robinson, and Paul B. Hopkins*
Department of Chemistry, University of Washington, Seattle, Washington 98195
Received March 14, 1989; Revised Manuscript Received July 5, 1989

ABSTRACT: A nitroxide spin-labeled analogue of thymidine (**1a**), in which the methyl group is replaced by an acetylene-tethered nitroxide, was evaluated as a probe for structural and dynamics studies of sequence specifically spin-labeled DNA. Residue **1a** was incorporated into synthetic deoxyoligonucleotides by using automated phosphite triester methods. ^{1}H NMR, CD, and thermal denaturation studies indicate that **1a** (T*) does not significantly alter the structure of 5′-d(CGCGAATT*CGCG) from that of the native dodecamer. EPR studies on monomer, single-stranded, and duplexed DNA show that **1a** readily distinguishes environments of different rigidity. Comparison of the general line-shape features of the observed EPR spectra of several small duplexes (12-mer, 24-mer) with simulated EPR spectra assuming isotropic motion suggests that probe **1a** monitors global tumbling of small duplexes. Increasing the length of the DNA oligomers results in significant deviation from isotropic motion, with line-shape features similar to those of calculated spectra of objects with isotropic rotational correlation times of 20-100 ns. EPR spectra of a spin-labeled GT mismatch and a T bulge in long DNAs are distinct from those of spin-labeled Watson-Crick paired DNAs, further demonstrating the value of EPR as a tool in the evaluation of local dynamic and structural features in macromolecules.

Improvements in the synthesis of sequence-defined DNA fragments have made possible the study of sequence-dependent properties of nucleic acids. Both single-crystal X-ray (Wing et al., 1980; Dickerson & Drew, 1981) and nuclear magnetic resonance (Wemmer et al., 1985) studies have revealed a remarkable sequence-dependent structural diversity within B-DNA. The likelihood that this structural variety is important in sequence-dependent recognition phenomena has engendered intense interest in this area. Several lines of evidence have recently suggested that sequence-dependent DNA *dynamics* might likewise be of biological importance. Spe-

† This work was supported in part by grants from the National Science Foundation (PCM-82-16762 and DMB-87-06175), the National Institutes of Health (GM 32681), and the Searle Scholars Program. P.B.H. is an NIH Research Career Development Award recipient (AG 00417).
* Address correspondence to this author.

0006-2960/89/0428-9484$01.50/0